High p_T Azimuthal Asymmetry in Non-central A+A at RHIC

Miklos Gyulassy[1,2], Ivan Vitev[1] and Xin-Nian Wang[2]
[1] *Dept. Physics, Columbia University, 538 W 120-th Street, New York, NY 10027*
[2] *Nuclear Science Division, Lawrence Berkeley National Lab, Berkeley, CA 94720*

The high $p_{\rm T} > 3$ GeV azimuthal asymmetry, $v_2(p_{\rm T})$, in non-central nuclear collisions at RHIC is shown to be a sensitive measure of the initial parton density distribution of the produced quark-gluon plasma. A generalization of the Gyulassy-Levai-Vitev (GLV) non-abelian energy loss formalism including Bjorken 1+1D expansion as well as important kinematic constraints is used.

PACS numbers: 12.38.Mh; 24.85.+p; 25.75.-q

arXiv:nucl-th/0012092v2 7 Mar 2001

Introduction. In order to interpret data on nuclear collisions from recent Relativistic Heavy Ion Collider (RHIC) experiments [1, 2, 3], it is obviously necessary to have knowledge of the *initial conditions*. Currently, there is an order of magnitude uncertainty in the initial produced gluon density, $\rho_g(\tau_0) \sim 10 - 100/\mathrm{fm}^3$, in central $Au + Au$ at $\sqrt{s} = 130$ AGeV since widely different models [4, 5] are consistent [6] with PHOBOS data [1]. We note that recent PHENIX data [3] appear to be inconsistent with at least one class (final state [5]) of gluon saturation models. It is essential, however, to check this with other observables as well. High $p_{\rm T}$ observables are ideally suited for this task because they provide a measure [4] of the total energy loss, ΔE, of fast partons, resulting from medium induced non-abelian radiation along their path [7, 8]. For intermediate jet energies ($E < 20$ GeV), the predicted [9, 10] gluon energy loss in a *static* plasma of density ρ_g and thickness, L is approximately $\Delta E_{GLV} \sim E(L/6\ \mathrm{fm})^2\rho_g/(10/\mathrm{fm}^3)$. The approximate linear dependence of ΔE on ρ_g is the key that enables high $p_{\rm T}$ observables to convey information about the initial conditions. However, ΔE also depends non-linearly on the geometry, L, of the plasma and therefore differential observables which have well controlled geometric dependences are also highly desirable.

A new way to probe ΔE in variable geometries was recently proposed in Ref. [11]. The idea is to exploit the spatial azimuthal asymmetry of non-central nuclear collisions. The dependence of ΔE on the path length $L(\phi)$ naturally results in a pattern of azimuthal asymmetry of high $p_{\rm T}$ hadrons which can be measured via the differential elliptic flow parameter (second Fourier coefficient), $v_2(p_{\rm T})$ [2]. In this letter, we predict $v_2(p_{\rm T} > 2\ \mathrm{GeV})$ for two models of initial conditions [6] which differ by an order of magnitude. We first generalize the finite energy GLV theory [9] to take into account the expansion (neglected in [10, 11]) of the produced gluon-dominated plasma while retaining kinematic constraints important for intermediate jet energies. Another novel element of the analysis is a discussion of the interplay between the azimuthally asymmetric soft (hydrodynamic [12]) and hard (quenched jet) components of the final hadron distributions. We show that the combined pattern of jet quenching in the single inclusive spectra and the differential elliptic flow at high $p_{\rm T}$ provide complementary tools that can determine the density as well as the spatial distribution of the quark-gluon plasma created at RHIC.

Hadron transverse momentum distributions. It is useful to decompose the nuclear geometry dependence of invariant hadron distributions produced in $A+B \to h+X$ at impact parameter $\mathbf{b}$ into a phenomenological "soft" and perturbative QCD (pQCD) calculable "hard" components as

$$dN_{AB}(\mathbf{b}) = N_{part}(\mathbf{b})\, dN_s(\mathbf{b}) + T_{AB}(\mathbf{b})\, d\sigma_h(\mathbf{b})\ , \qquad (1)$$

where $N_{part}(\mathbf{b})$ is the number of nucleon participants, and $T_{AB}(\mathbf{b}) = \int d^2\mathbf{r}\ T_A(\mathbf{r})T_B(\mathbf{r}-\mathbf{b})$ is the Glauber profile density per unity area in terms of nuclear thickness functions, $T_A(\mathbf{r}) = \int dz\ \rho_A(\mathbf{r}, z)$. The computable lowest order pQCD differential cross section for inclusive $p + p \to h + X$ production is given by

$$E_h \frac{d\sigma_h^{pp}}{d^3p} = K \sum_{abcd} \int dx_a dx_b f_{a/p}(x_a, Q_a^2) f_{b/p}(x_b, Q_b^2) \frac{d\sigma}{d\hat{t}}(ab \to cd) \frac{D_{h/c}(z_c, Q_c^2)}{\pi z_c}\ , \qquad (2)$$

where x_a, x_b are the initial parton momentum fractions, $z_c = p_h/p_c$ is the final hadron momentum fraction, $f_{a/p}(x_a, Q_a^2)$ are the parton distribution functions and $D_{h/c}(z_c, Q_c^2)$ is the fragmentation function for $c \to h$. The UA1 data on $p\bar{p}$ hadron production with $p_{\rm T} > 1$ GeV can be well reproduced with the above formula using $Q^2 = p_{\rm T}^2/2$, $K = 2$ and Martin-Roberts-Sterling [13] (MRSD-') structure functions.

In nuclear collisions jet quenching can modify the hard cross section by changing the kinematic variables of the effective fragmentation function. We follow Ref. [11] and include this effect by replacing the vacuum fragmentation function in Eq. (2) by an effective quenched one

$$z_c D'_{h/c}(z_c, Q_c^2) = z'_c D_{h/c}(z'_c, Q_{c'}^2) + N_g z_g D_{h/g}(z_g, Q_g^2)\ ,$$
$$z'_c = \frac{p_h}{p_c - \Delta E_c(p_c, \phi)}\ , \quad z_g = \frac{p_h}{\Delta E_c(p_c, \phi)/N_g}\ , \qquad (3)$$

where z'_c, z_g are the rescaled momentum fractions. The first term is the fragmentation function of the jet c after losing energy $\Delta E_c(p_c, \phi)$ due to medium *induced* gluon radiation. The second term is the feedback due to the fragmentation of the $N_g(p_c, \phi)$ radiated gluons. The

modified fragmentation function satisfies the sum rule $\int dz_c\, z_c D'_{h/c}(z_c, Q_c^2) = 1$.

Energy loss in a longitudinally expanding plasma. The GLV reaction operator formalism [9] expands the radiative energy loss formally in powers of the mean number, χ, of interactions that the jet of energy E suffers along its path of propagation through dense matter. For a jet produced at point $\vec{x}_0$, at time τ_0, in an *expanding* and possibly azimuthally asymmetric gluon plasma of density $\rho(\vec{x}, \tau)$, the opacity in direction $\hat{v}(\phi)$ is

$$\chi(\phi) = \int_{\tau_0}^{\infty} d\tau\ \sigma(\tau)\rho(\vec{x}_0 + \hat{v}(\phi)(\tau - \tau_0), \tau)\ . \qquad (4)$$

Note that the gluon-gluon elastic cross section, $\sigma(\tau) = 9\pi\alpha_s^2/2\mu_{eff}^2(\tau)$, and the density may vary along the path. For a finite jet energy, E, the approximate upper kinematic bound of medium induced momentum transfers is $|\mathbf{q}(\tau)_{\rm max}| \approx \sqrt{3\mu(\tau)E}$ and $\mu_{eff}^2(\tau) = \mu^2(\tau)(1 + \mu^2(\tau)/\mathbf{q}^2(\tau)_{\rm max})$. The explicit closed form expression for the $n^{\rm th}$ order opacity expansion of the gluon radiation double differential distribution for a static medium is given in Ref. [9]. Fortunately, the opacity expansion converges very rapidly due to the formation time physics, and the first order term was found to give the dominant contribution. Higher order corrections decrease rapidly with energy. All numerical results in this letter include $2^{\rm nd}$ and $3^{\rm rd}$ order correction factors computed in the static plasma limit [9]. We also include finite kinematic bounds on the transverse momentum, $\mathbf{k}^2_{\rm max} = \min\left[4E^2x^2, 4E^2x(1-x)\right]$ and $\mathbf{k}^2_{\rm min} = \mu^2$, for gluons with light-cone momentum fraction x. Finite kinematics reduces energy loss at intermediate jet energies [9, 10] as compared to the asymptotic formalism [8].

The dominant (generalized) first order radiation *intensity* distribution [9] that holds also for expanding plasmas is given by ($z = \tau$)

$$\frac{dI^{(1)}}{dx} = \frac{9C_R E}{\pi^2}\int_{z_0}^{\infty} dz\,\rho(z)\int^{|\mathbf{k}|_{\rm max}} d^2\mathbf{k}\,\alpha_s\int^{|\mathbf{q}|_{\rm max}}\frac{d^2\mathbf{q}\ \alpha_s^2}{(\mathbf{q}^2+\mu(z)^2)^2}$$
$$\frac{\mathbf{k}\cdot\mathbf{q}}{\mathbf{k}^2(\mathbf{k}-\mathbf{q})^2}\left[1-\cos\left(\frac{(\mathbf{k}-\mathbf{q})^2}{2xE}(z-z_0)\right)\right]\ . \qquad (5)$$

In order to compare to previous asymptotic results [8] for expanding plasmas, consider a density of the form

$$\rho(z) = \rho_0\left(\frac{z_0}{z}\right)^{\alpha}\theta(L-z)\ , \qquad (6)$$

where $\alpha = 0$ corresponds to a static uniform medium of thickness L, while $\alpha = 1$ to a more realistic Bjorken 1+1D expansion of the plasma (transverse to the jet propagation axis). Analytic expressions can be obtained only for asymptotic jet energies when the kinematic boundaries can be ignored [8]. If we set $\mathbf{q}^2_{\rm max} = \mathbf{k}^2_{\rm max} = \infty$, neglect the running α_s and change variables $\mathbf{k} - \mathbf{q} \to \mathbf{k}$, $u = \mathbf{k}^2/\mu^2(z)$ and $w = \mathbf{q}^2/\mu^2(z)$, then Eq. (5) reduces to

$$\frac{dI^{(1)}}{dx} = E\,\frac{2C_R\alpha_s}{\pi}\int_{z_0}^{\infty} dz\,\sigma(z)\rho(z)\ f(Z(x,z))\ , \qquad (7)$$

where $Z(x,z) = (z - z_0)\mu^2(z)/2xE$ and

$$f(x,z) = \int_0^{\infty}\frac{du}{u(1+u)}\left[1-\cos\left(\,uZ(x,z)\right)\right]$$
$$\approx \frac{\pi Z}{2} + \frac{Z^2}{2}\log(Z) + \mathcal{O}(Z^2)\ . \qquad (8)$$

For a target of thickness L, the small $Z(x,z)$ limit applies as long as $x \gg x_c = L\mu^2(L)/2E$. In that domain $dI/dx \propto 1/x$. For $x \ll x_c$, $f(Z) \approx \log Z$ and $dI/dx \propto \log 1/x$ is integrable to $x = 0$.

By integrating over x, the total energy loss is

$$\Delta E = E\frac{2C_R\alpha_s}{\pi}\int_0^1 dx\int_{z_0}^{\infty} dz\,\sigma(z)\rho(z)\ f(Z(x,z))$$
$$\approx \frac{C_R\alpha_s}{2}\int_{z_0}^{\infty} dz\,\frac{\mu^2(z)}{\lambda(z)}\ (z-z_0)\log\frac{E}{\mu(z)}\ , \qquad (9)$$

which is an approximately linearly weighed line integral over the local transport coefficient $(\mu^2(z)/\lambda(z))\log E/\mu(z) = 9\pi\alpha_s^2\rho(z)\tilde{v}/2$. For a uniform and expanding plasma as in (6)

$$\Delta E_\alpha(L, z_0) \approx \frac{C_R\alpha_s}{2}\left(\frac{\mu^2(z_0)z_0^\alpha}{\lambda(z_0)}\right)\left(\frac{L^{2-\alpha} - z_0^{2-\alpha}}{2-\alpha}\right)\tilde{v}$$
$$= \frac{C_R\alpha_s}{2}\frac{\mu^2(L)L^\alpha}{\lambda(L)}\ \frac{L^{2-\alpha}}{2-\alpha}\,\tilde{v}\ . \qquad (10)$$

Here $\tilde{v} = \log E/\mu$ and we used that $\mu^2(L)L^\alpha/\lambda(L)$ is a constant independent of L for this type of expansion and took the $z_0 \to 0$ limit. We therefore recover the asymptotic Baier-Dokshitzer-Mueller-Schiff (BDMS) and Zakharov (Z) energy loss for both static and expanding media [8]. We note that for Bjorken expansion, the asymptotic energy loss can be expressed in terms of the initial gluon rapidity density as

$$\Delta E_{\alpha=1}(L) = \ \frac{9C_R\pi\alpha_s^3}{4}\left(\frac{1}{\pi R^2}\frac{dN^g}{dy}\right)\ L\,\log\frac{E}{\mu}\ . \qquad (11)$$

If we vary $L = R \propto A^{1/3}$ by varying the nuclear size, then nonlinearity in L arises because $dN^g/dy \propto A^{1+\delta}$. For HIJING initial conditions [4] $\delta = 1/3$, while in the EKRT saturation model [5] $\delta \approx 0$.

Implications of nuclear geometry. For nucleus-nucleus collisions the co-moving plasma produced in an $A + B$ reaction at impact parameter $\mathbf{b}$ at formation time $\tau = z_0$ has a transverse coordinate distribution given by

$$\rho_g(\mathbf{r}, z = 0, \tau = z_0) = \frac{1}{z_0}\frac{d\sigma^{\rm jet}}{dy}\,T_A(\mathbf{r})\,T_B(\mathbf{r}-\mathbf{b})\ , \qquad (12)$$

where $d\sigma^{\rm jet}/dy$ is the pQCD mini-jet cross section in pp collisions at a given $\sqrt{s}$. Note that taking into account also the 2D transverse expansion causes the density to decrease somewhat faster than Eq. (6). However, we found numerically that transverse expansion can be ignored in the first approximation.

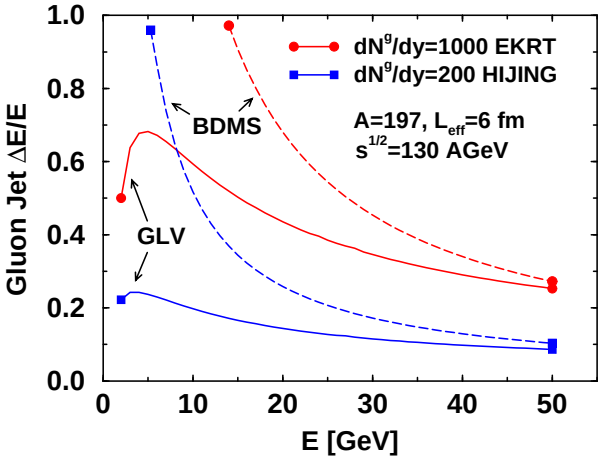

FIG. 1. The GLV fractional energy loss in Bjorken expanding gluon plasma with [4, 5] $dN^g/dy \simeq 200, 1000$.

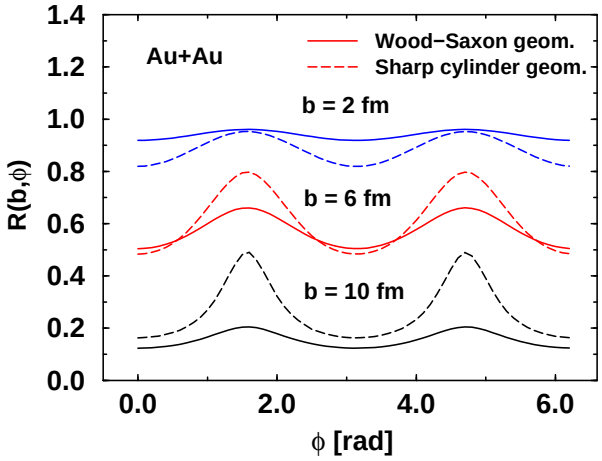

FIG. 2. The modulation function $R(\mathbf{b}, \phi)$ is plotted vs. ϕ for several impact parameters.and Wood-Saxon vs cylinder geometries.

In the linear $f(Z) \approx \pi Z/2$ (8) and Bjorken approximations, the total energy loss is proportional to the line integral (7,9) along the jet trajectory $\mathbf{r}(z, \phi) = \mathbf{r} + \hat{v}(\phi)(z - z_0)$, averaged over the distribution of the jet production points

$$F(\mathbf{b}, \phi) = \int d^2\mathbf{r}\, \frac{T_A(\mathbf{r}) T_B(\mathbf{r} - \mathbf{b})}{T_{AB}(\mathbf{b})} \int_{z_0}^{\infty} dz\, z\, \left(\frac{z_0}{z}\right)^{\alpha} T_A(\mathbf{r}(z, \phi)) T_B(\mathbf{r}(z, \phi) - \mathbf{b}) \,, \quad (13)$$

where $T_A(\mathbf{r}), T_B(\mathbf{r} - \mathbf{b})$ and $T_{AB}(\mathbf{b})$ depend on the geometry. In particular, for a sharp uniform cylinder of radius $R_{\rm eff}$ one readily gets $T_A(\mathbf{r}) = (A/\pi R_{\rm eff}^2)\theta(R_{\rm eff} - |\mathbf{r}|)$ and $T_{AB}(0) = A^2/\pi R_{\rm eff}^2$. We can therefore define the effective radius of the sharp cylinder equivalent to a diffuse Wood-Saxon geometry via

$$F(\mathbf{0}, \phi)_{\rm Wood-Saxon} = F(\mathbf{0}, \phi)_{\rm Sharp\ \ cylinder} \,. \quad (14)$$

For $Au + Au$ collisions and $\alpha = 1$, Eq. (14) gives $R_{\rm eff} \approx 6$ fm. Eq. (5) can then be integrated numerically to give $\Delta E(0)/E$, allowing α_s to run and including kinematical bounds. Fig. 1 illustrates the fractional energy loss for gluon jets at $b = 0$ for a broad range of initial gluon densities [4, 5].

For a non-vanishing impact parameter $\mathbf{b}$ and jet direction $\hat{v}(\phi)$, we calculate the energy loss as

$$\frac{\Delta E(\mathbf{b}, \phi)}{E} = \frac{F(\mathbf{b}, \phi)}{F(\mathbf{0}, \phi)} \frac{\Delta E(0)}{E} \equiv R(\mathbf{b}, \phi) \frac{\Delta E(0)}{E} \,, \quad (15)$$

where the modulation function $R(\mathbf{b}, \phi)$ captures in the *linearized* approximation the $\mathbf{b}$ and ϕ dependence of the jet energy loss. Fig. 2 shows the $R(\mathbf{b}, \phi)$ modulation factor plotted against the azimuthal angle ϕ for impact parameters $\mathbf{b} = 2, 6, 10$ fm. Note that $R(\mathbf{b}, \phi)$ reflects not only the dimensions of the characteristic "almond" cross section shape of the interaction volume but also the rapidly decreasing initial plasma density as a function of the impact parameter.

Phenomenological soft "hydrodynamic" component. In order to compare to the new STAR data [2] at $p_{\rm T} < 2$ GeV, we must also take into account the soft non-perturbative component that cannot be computed with the eikonal jet quenching formalism above. In [11] this was simply modeled by an azimuthally *symmetric* exponential form. However, in non-central A+B reactions the low $p_{\rm T}$ hadrons are also expected to exhibit azimuthal asymmetry caused by hydrodynamic like flow effects [12]. We therefore model the low $p_{\rm T}$ soft component here with the following ansatz:

$$\frac{dN_s(\mathbf{b})}{dy d^2\mathbf{p}_{\rm T}} = \frac{dn_s}{dy} \frac{e^{-p_{\rm T}/T_0}}{2\pi T_0^2} (1 + 2v_{2s}(p_{\rm T}) \cos(2\phi)) \,, \quad (16)$$

where we take $T_0 \approx 0.25$ GeV and incorporate the hydrodynamic elliptic flow predicted in [12] and found to grow monotonically with $p_{\rm T}$ as

$$v_{2s}(p_{\rm T}) \approx \tanh(p_{\rm T}/(10 \pm 2\ {\rm GeV})) \,. \quad (17)$$

It is important to emphasize that hydrodynamic flow was found [12] to be less sensitive to the initial conditions than the high p_T jet quenching reported here.

With the inclusion of this non-perturbative soft component, it follows from Eq. (1) that the effective differential flow is

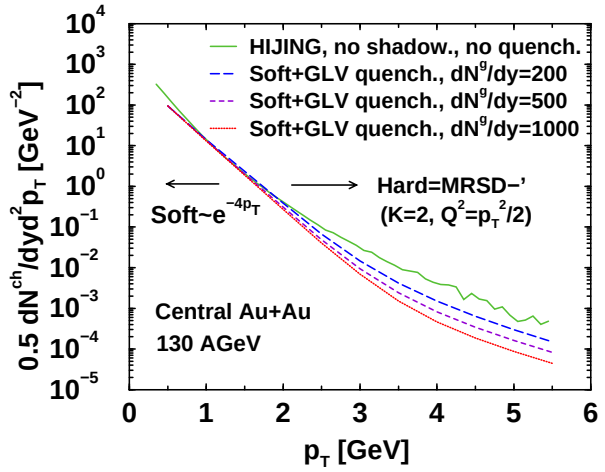

FIG. 3. Sensitivity of central-collision inclusive hadron distributions to initial conditions and energy loss in the two component hydrodynamic + quenched jet model.

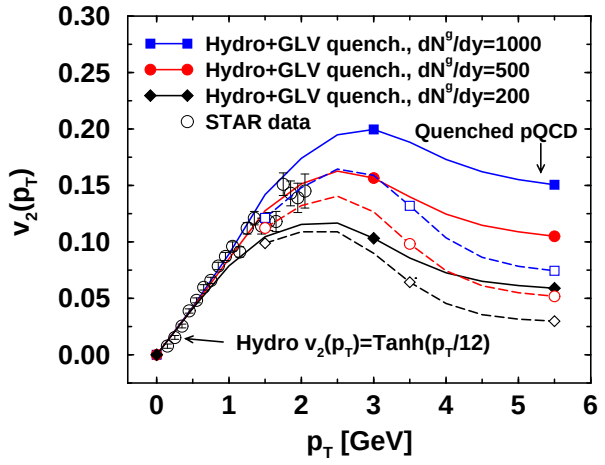

FIG. 4. The interpolation of $v_2(p_{\rm T})$ between the soft hydrodynamic [12] and hard pQCD regimes is shown for $b = 7$ fm. Solid (dashed) curves correspond to cylindrical (Wood-Saxon) geometries.

$$v_2(p_{\rm T}) \approx \frac{v_{2s}(p_{\rm T})dN_s + v_{2h}(p_{\rm T})dN_h}{dN_s + dN_h} \,. \qquad (18)$$

This interpolates between the hydrodynamic and the pQCD regimes because at high $p_{\rm T}$, $dN_h \gg dN_s$. For our numerical estimates the low $p_{\rm T}$ interpolation is achieved by multiplying the pQCD curves with a switch function $[1 + \tanh(3(p_{\rm T} - 1.5\,{\rm GeV}))]/2$.

Conclusions. Fig. 3 shows the inclusive charged particle transverse momentum distribution in central $Au+Au$ collisions with three models of initial gluon densities $dN^g/dy = 1000, 500, 200$. We see that jet quenching can be disentangled from the soft hydrodynamic component only for transverse momenta $p_{\rm T} > 4$ GeV. In that high $p_{\rm T}$ region there is an approximately constant suppression relative to the unquenched (HIJING) distribution due to the approximately *linear* energy dependence [10] of the GLV energy loss [9]. The suppression increases systematically with increasing initial plasma density and thus provides an important constraint on the maximum initial parton densities produced in $\mathbf{b} = 0$ collisions.

Fig. 4 shows the predicted pattern of high $p_{\rm T}$ anisotropy. Note the difference between sharp cylinder and diffuse Wood-Saxon geometries at $\mathbf{b} = 7$ fm, the characteristic impact parameter of minimum bias events. While the central ($\mathbf{b} = 0$) inclusive quenching is insensitive to the density profile (due to Eq. (14)), non-central events clearly exhibit large sensitivity to the actual distribution. We checked numerically that transverse expansion with $v_\perp = 0.5c$ can be ignored since it reduces the jet quenching effects in Figs. 3,4 by <20% at high $p_{\rm T}$.

We conclude that $v_2(p_{\rm T} > 2\ {\rm GeV}, \mathbf{b})$ provides essential complementary information about the geometry and impact parameter dependence of the initial conditions in $A + A$. In particular, the rate at which the v_2 coefficient decreases at high $p_{\rm T}$ is an indicator of the diffuseness of that geometry.

We thank P. Huovinen, R. Snellings, A. Poskanzer, and H.J. Ritter for stimulating discussions. This work was supported by the the U.S. DOE under DE-AC03-76SF00098 and DE-FG-02-93ER-40764 and by the NSFC under No. 19928511.

[1] B.B. Back *et al.* [PHOBOS Collaboration], Phys. Rev. Lett. **85**, 3100 (2000) [hep-ex/0007036].
[2] K.H. Ackermann *et al.* [STAR Collaboration], Phys. Rev. Lett. **86**, 402 (2001) [nucl-ex/0009011].
[3] C. Adcox *et al.*, [PHENIX Collaboration], nucl-ex/0012008.
[4] X.-N. Wang and M. Gyulassy, Phys. Rev. Lett. **68** 1480 (1992); M. Gyulassy and M. Plümer, Phys. Lett. **B243** 432 (1990).
[5] K.J. Eskola, K. Kajantie, P.V. Ruuskanen, K. Tuominen, Nucl. Phys. **B570** 379 (2000).
[6] X.-N. Wang and M. Gyulassy, nucl-th/0008014.
[7] M. Gyulassy and X.-N. Wang, Nucl. Phys. **B420** 583 (1994).
[8] R. Baier, Y.L. Dokshitzer, A.H. Mueller and D. Schiff, Phys. Rev. **C60** 64902 (1999); B.G. Zhakharov, JETP Lett. **65** (1997) 615; U.A. Wiedemann, Nucl. Phys. **B588** 303 (2000)
[9] M. Gyulassy, P. Lévai and I. Vitev, Nucl. Phys. **B594** 371 (2001); Phys. Rev. Lett. **85** 5535 (2000).
[10] X.-N. Wang, Phys. Rev. C **61**, 064910 (2000); P. Levai, G. Papp, G. Fai and M. Gyulassy, nucl-th/0012017.
[11] X.-N. Wang, nucl-th/0009019, Phys. Rev. C to appear.
[12] J.Y. Ollitraut, Phys. Rev. **D46** (1992) 229; P.F. Kolb, P. Huovinen, U. Heinz and H. Heiselberg, hep-ph/0012137.
[13] A.D. Martin, R.G. Roberts, W.J. Stirling, Phys. Lett **B306** 147 (1993).